



ELSEVIER

Available online at www.sciencedirect.com

ScienceDirect

journal homepage: www.elsevier.com/locate/he

Detection of liquid water in the flow channels of PEM fuel cell using an optical sensor

Kristopher Inman, Xia Wang*

Department of Mechanical Engineering, Oakland University, Rochester, MI 48309, USA

ARTICLE INFO

Article history:

Received 18 June 2014

Received in revised form

9 September 2014

Accepted 26 September 2014

Available online 14 October 2014

Keywords:

Proton exchange membrane fuel cells

Optical sensor

Temperature measurement

Liquid water

ABSTRACT

An optical sensor was developed with the capability of detecting liquid water in the flow channels of a proton exchange membrane fuel cell (PEMFC) as well as simultaneously measuring temperature. This work is an extension of previous research in which an optical temperature sensor was developed for measuring the in situ temperature of PEM fuel cells based on the principles of phosphor thermometry. The optical sensor was installed in the cathode flow channel of a 5 cm² proton exchange membrane fuel cell. The fuel cell was tested under both dry and humid conditions. Liquid water formation in the flow channels was quantitatively measured from the experimental data. An observed time fraction value was estimated for characterizing flow channel flooding. The observed time fraction of liquid water in the flow channel was found to be closely related to the relative humidity of reactants and the operating current of the fuel cell.

Copyright © 2014, Hydrogen Energy Publications, LLC. Published by Elsevier Ltd. All rights reserved.

Introduction

Water management in proton exchange membrane (PEM) fuel cells has been difficult to study experimentally due to a limited number of experimental methods. This has arguably led to a minimum understanding of water management in PEMFCs as well as made two-phase numerical models difficult to validate. Poor water management can cause decreased fuel cell performance by choking of the cathode catalyst layer with liquid water, which is manifested as a decrease in power at higher current densities. Liquid water formation in flow channels can also obstruct and reduce reactant flow to locations inside of a fuel cell as well as increase pressure head into the fuel cell stack. In order to overcome these deficiencies proper water management is critical. However, water management can be difficult to measure or characterize in the field

or in mobile applications outside of the laboratory, due to a lack of experimental methods currently available for PEMFCs. Because of the relatively small geometry of fuel cell components and the acidic environment of its active components, the development of diagnostic tools to perform liquid water detection and measurement which can be integrated into the fuel cell system itself is challenging.

Few experimental methods have been developed that can directly measure liquid water formation in flow channels of fuel cell stacks without significant modification or design considerations. One of these methods was developed by Conteau et al. [1] who created an electrical micro-sensor for the detection of liquid water in the flow channels of PEMFCs. The sensor they developed was based on the principle of changing electrical impedance between two electrodes created by a water droplet passing between them. While a promising technique, the authors had presented the operation

* Corresponding author. Tel.: +1 248 370 2224; fax: +1 248 370 4416.

E-mail address: wang@oakland.edu (X. Wang).

<http://dx.doi.org/10.1016/j.ijhydene.2014.09.149>

0360-3199/Copyright © 2014, Hydrogen Energy Publications, LLC. Published by Elsevier Ltd. All rights reserved.

of the sensor in an experimental cell that was non-functional but represented a PEMFC. David et al. [2] developed an optical sensor for the measurement of humidity in PEMFCs with the use of Bragg optical fibers. While being able to measure relative humidity in the cell, these sensors were not capable of point measurement or detection of liquid water. Nishida et al. [3] created a method of measuring water generation in PEMFCs using water sensitive paper. While this method was shown to have no significant influence on PEMFC performance, it requires the cell to operate at low current densities and for short periods of time. Furthermore, the installation and removal of the paper before it becomes saturated making it difficult to use in applications outside of the laboratory.

A common method for the detection and quantification of liquid water in PEMFCs is the use of optically transparent cells [4–8]. Optical fuel cells allow for the observation of liquid water, typically on the cathode side, of a single cell by creating a window in one side which allows for the component of interest to be visually observed or photographed. This can involve combining the cathode flow plate and current collector into a single component backed by an optical window [4,6]. However, this level of modification can have a large impact on electrical conductivity and contact resistance as well as changes in thermal behavior. Many designs such as work in Refs. [7,8] include an optical window constructed of polycarbonate and other plastics. Polycarbonate and other polymers slowly deform under mechanical stress and are not capable of providing uniform and constant pressure over the MEA, especially at elevated temperatures. While simple and effective, these levels of modifications often make the physical phenomenon to be analyzed non-representative of what might actually occur in a more conventionally designed fuel cell.

Much work has been performed with the use of nuclear magnetic resonance (NMR) and beam interrogation techniques, such as neutron radiography [9–11] and X-ray radiography [12], for the detection of liquid water in PEMFCs. While these techniques have been proven to be excellent diagnostic tools with increasingly high resolution in space or time, they do have many shortcomings. NMR, neutron radiography, and X-ray imaging all require equipment that practically should be used in a laboratory setting or is of limited availability [13]. Furthermore, specific materials must be used for the construction of the fuel cells to be studied in order to be compatible with the devices and techniques [14].

One of the most common methods for studying water transport in PEMFCs is with two-phase numerical modeling [15–19]. Due to the complex physics and unknown or estimated physical parameters, validating these two-phase models is often difficult. It is highly advantageous to have a method which not only allows the detection of liquid water droplets in the flow channels of PEMFCs but also provides the capability of quantifying water content for use in validating theoretical models. Especially of interest are models that have been developed which discretely model water droplet formation and transport in PEMFC flow channels like those developed by Ding et al. [20].

In summary, it is very critical to find a simple and minimally invasive method to detect water generation in the PEM fuel cell. The objective of this work is to develop a method for

the detection of water formation in the flow channels and quantify that information so that it may be useful in better understanding water management and possibly provide a validation to two-phase models. The method demonstrated in this work can minimally-invasively detect liquid water movement at a single point in the flow channels of a PEMFC using an optical sensor. Furthermore, a method is also proposed for quantifying these measurements for the means of measuring a liquid water time fraction or to create a probability density function of finding liquid water in the flow channel at any given point in time. This then can be used for theoretical model development and validation under a variety of operating conditions. The optical sensor used in this work is an adaptation of an earlier developed sensor where the in situ temperatures of a PEMFC were measured using the life-time decay method of phosphor thermometry [21,22].

Principles of operation and design

Phosphor thermometry is an optical temperature measurement method which uses the thermo-luminescent properties of phosphors to determine temperature on the surface of an object. It involves exciting a phosphor material applied to the surface to be analyzed using a light source or heat and then observing the radiative emission over time once the excitation source has been removed. Because phosphors are electrically non-conductive and chemically inert, phosphor thermometry is an ideal method of temperature measurement inside of PEM fuel cells. Our previous work [21,22] has shown that the sensor does not have a measurable impact on PEMFC performance or behavior.

The optical sensor developed in previous work involved embedding two optical fibers in the cathode flow channel plate of a PEM fuel cell with a phosphor material applied to the surface of the gas diffusion layer (GDL) as shown in Fig. 1. Given that a rather small amount of phosphor material is applied to the surface and that it is non-soluble in water, it is not expected or observed to alter the hydrophobic properties of the GDL is applied to. The phosphor is in optical contact with the fiber but gas and water are allowed to flow between the fibers and the phosphor. This allows for a “remote” temperature measurement of the GDL surface without obstructing liquid or gas flow inside of the cell.

Method of water detection

When the sensor is measuring temperature, light is emitted from a blue LED (~470 nm) and is collimated into a 0.5 mm diameter optical fiber which is in optical view of the phosphor material applied to the GDL. This optical fiber is used for exciting the phosphor material. When this light from the LED is removed, the phosphor emits light in the red color spectrum (~687 nm) which is carried to a photodetector using a 1 mm diameter optical fiber which is placed adjacent to the 0.5 mm diameter fiber used for excitation of the phosphor. When the phosphor is excited with a repeated pulse at a high enough frequency the emission signal from the photodetector takes the form of a semi-sinusoidal waveform as shown as v_{em} in Fig. 2.

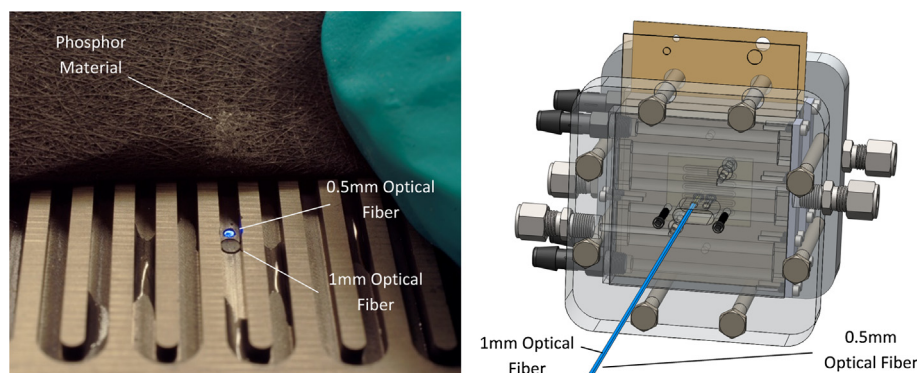


Fig. 1 – Image of optical sensor installed in an experimental fuel cell (Left). CAD image of experimental fuel cell showing optical fiber placement (Right).

This emission response of phosphor has a difference in phase from the excitation waveform labeled as v_{ex} . The phase lag of this waveform, labeled as ϕ , is dependent upon temperature, while the amplitude of this signal is dependent upon the amount of light emitted from the phosphor that is detected. When the light is absorbed and emitted from the phosphor unimpeded, the amplitude of the signal is the strongest, as is the case with a dry channel containing only gas. However, when liquid water is present in the channel between the optical fiber and the phosphor, light is attenuated due to reflection, diffraction, and scattering. The end result of this is a detected waveform with lower amplitude labeled as α , shown in Fig. 2. In summary, from this one signal, temperature of the phosphor is determined due to a phase lag while liquid water is observed through signal amplitude. Both of these measurements are independent of each other but both sets of information can be obtained from the single signal simultaneously. Because the excitation source is an LED, the amount of energy light from the sensor is estimated to be approximately about 42 mW per pulse (21 mW avg) with about 5 mW being re-emitted by the phosphor. This amount of energy is considered negligible given the amount of heat produced by the fuel cell and thermally conductivity of the materials. Furthermore, calibration of temperature

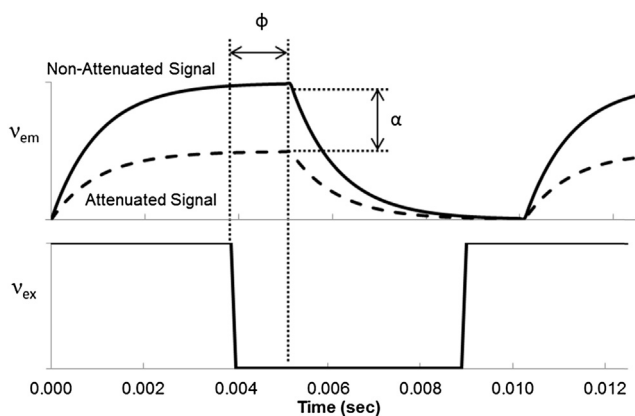


Fig. 2 – Example of excitation and emission waveforms generated by optical sensor.

measurement, shown in our previous publications [21,22], shows no measurable influence of heat generated by the sensor.

Fig. 3 shows the placement of the two optical fibers in the flow channel plate along with the location of the phosphor on the GDL. The left part of Fig. 3 shows the behavior of the emission signal magnitude when the channel is dry and contains no liquid water. The amount of signal attenuation remains constant with no abrupt changes. The right side of Fig. 3 shows the behavior of the emission signal as water droplets form or move through the flow channel. As the droplets pass between the fibers and the phosphor, light is reflected or scattered as it moves through the water droplet to the phosphor, and back through the water droplet to the receiving fiber. This typically causes a decrease in signal magnitude, however depending on the size and shape of the water droplet, lensing can occur as well creating an increased signal magnitude. Ultimately, an abrupt change in signal magnitude is observed over the period of time when liquid water is located between the fibers and phosphor. One important characteristic of the sensor is that while it is able to detect liquid water in slug or droplet form, it is incapable of determining the shape or volume of water slugs or droplets. Therefore the method in this work is strictly a statistical method and not an explicit one as it is incapable of actually measuring volumes of liquid water. Only the presence of liquid water at the sensor can be determined and not a quantification of the amount. Therefore, the observed time fraction value is not a measurement of the saturation of the flow channel volume, but the saturation at the GDL and flow channel interface or boundary.

System design and data acquisition

The sensor system, shown in Fig. 4, consists of the phosphor and optical fibers which are embedded in the fuel cell, along with other optical and electronic hardware. The excitation part of the sensor system consists of a high power blue LED controlled by a driver circuit and microcontroller. Light from the LED is collimated into the 0.5 mm optical fiber using an aspheric lens. The detection portion of the circuit consists of an avalanche photodiode (APD) as the photodetector which

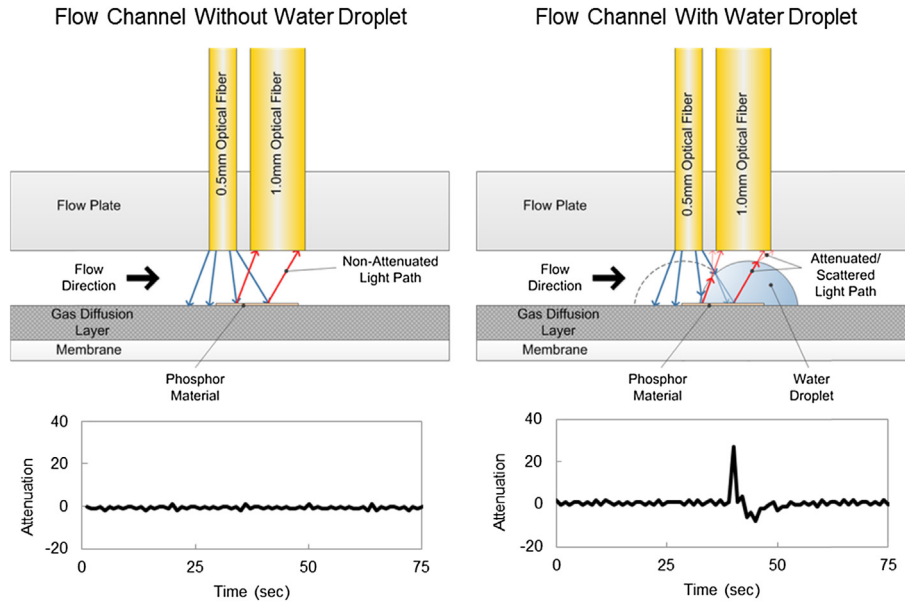


Fig. 3 – Diagram of sensor placement and influence of liquid water movement on sensor signal attenuation.

receives the emitted light from the phosphor (687 nm) through the larger 1 mm diameter optical fiber. The photodetector includes a band-pass filter between the optical fiber and the APD to reject blue light from the excitation source. An aspheric lens is used to focus light from the fiber and filter onto the avalanche photodiode.

An electronic circuit was developed to measure the magnitude of the emission signal being received from the photodetector over time. The principal component of the water detection circuit is a RMS to DC voltage converter. The voltage signal from the photodetector circuit is amplified and then fed to a high pass filter to remove the DC component of the signal. It is then fed to the RMS to DC voltage converter where the DC voltage is measured using an analog to digital converter (ADC) on the microcontroller. The ADC is capable of sampling at rate of 500 kHz which is more than

capable of detecting even the theoretically fastest water droplet with a dwell time of 0.3 ms based on a maximum gas velocity of 7 m s^{-1} for a 2 mm of detection length. Based on the initial development of this sensor and work performed by Conteau et al. [1], liquid water droplets were found to have dwell times of many seconds and therefore such high sampling rates are not required. Information from the microcontroller is then transferred to a PC running an MS Excel based interface program where signal amplitude, time, and temperature are recorded. The water measurement system is capable of sampling data at a rate of up to 100 Hz. However, given the typical water droplet dwell time, and practical file size, a sample rate of 1 Hz is used for all data collected in this paper. The lock-in amplifier shown in Fig. 4 is to support the simultaneous temperature measurement function.

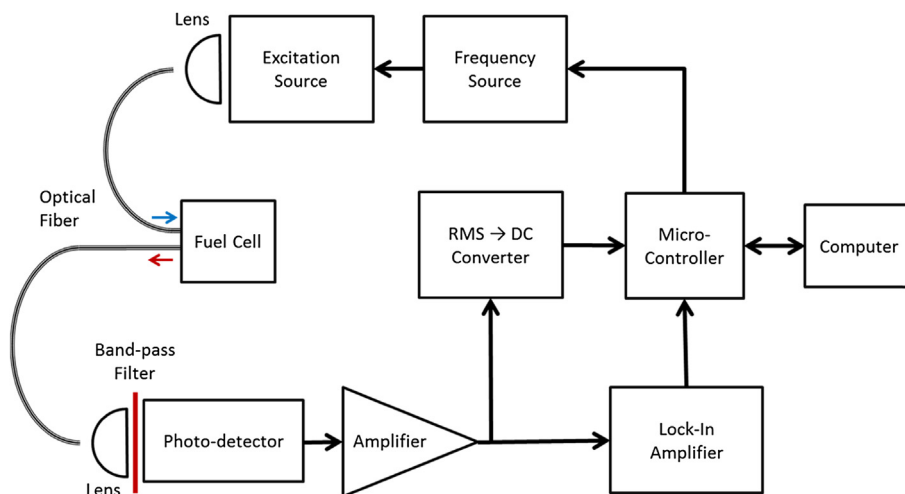


Fig. 4 – System diagram of optical water detection sensor including RMS to DC converter for attenuation measurement.

Concept of time fraction measurement

The optical sensor is only capable of detecting the presence of liquid water at its location. It is not capable of determining the size or shape of water droplets themselves or if the channel is completely filled. Therefore, the change in amplitude of the signal received from the phosphor can only be used to satisfy a Boolean condition, whether there is liquid water at the location of the sensor represented by a value of “1”, or if the channel is dry then it is represented with a value of “0”. This is determined by observing the time trace of the amplitude of the emission signal and identifying the amount of time when liquid water is observed in the channel and the time when it is not.

The presence of liquid water is identified by looking for abrupt changes in the transient plot of signal amplitude. A dry channel will record no changes in amplitude with the exception of a small amount of consistent noise generated by the photodetector and other electronic components. However, when a water droplet enters the location of the sensor, an abrupt increase or decrease in amplitude will occur. The period over which these changes occur is the time at which liquid water is present at the sensor. All other times are considered to be dry and are assigned a value of 0. To mathematically decipher when a single measurement should be a 1 or 0, the noise of the signal is analyzed and characterized. More specifically, a moving standard deviation of a small number of samples is calculated and this standard deviation is compared to the baseline noise of the signal. If the standard deviation is within the limit of the baseline noise it is assumed to be a dry condition, while all other values of the standard deviation which exceed the noise limit are assigned as 1. An example of an amplitude signal that has been analyzed is shown in Fig. 5.

Method for quantifying the liquid time fraction

Using the definition of the mean value theorem in integral form and the definition of the mean for a discrete sample size, the liquid water time fraction, F , can be defined by numerically

integrating the sampled condition of the flow channel, f , over an infinite amount of time as shown in Equation (1).

$$F = \lim_{N \rightarrow \infty} \frac{1}{N} \sum_{i=1}^N f_i = \frac{1}{T} \int_0^{\infty} f dt \quad (1)$$

Since measuring and sampling the discrete time value over an infinite period of time is impractical, a finite amount of samples are required in order to make an approximation to the true average liquid time fraction.

$$F \approx \bar{f} = \frac{1}{N_T} \sum_{i=1}^{N_T} f_i \quad (2)$$

The liquid water time fraction is approximated by averaging the discrete time value over time. However, the issue arises of how many measurements are required in order to make a reasonably accurate approximation.

To determine the number of measurements required for a suitable approximation, a statistical analysis was performed using experimental data from preliminary experiments. A confidence interval, E , is established along with a level of desired confidence value for the measurement, z_{CV} . The value of z_{CV} used for this calculation is taken from the standard normal distribution. While the probability distribution of F is a binomial distribution, the sample size is large and therefore continuity correction is used to approximate the value of z_{CV} .

The above statistical information is used with Equation (3) to determine the number of samples required to approximate the liquid time fraction within the confidence interval.

$$N_T = \left(\frac{z_{CV} S_1}{E} \right)^2 \quad (3)$$

The value S_1 is the standard deviation of the sample values from preliminary experiments and N_T the total number of required measurements. The total value of required samples, or the required amount of measurement time, is a function of the variance of the discrete time value along with the desired confidence interval and confidence value. In preliminary experiments it was found that the variance of the discrete time value changed depending on the operating conditions of the

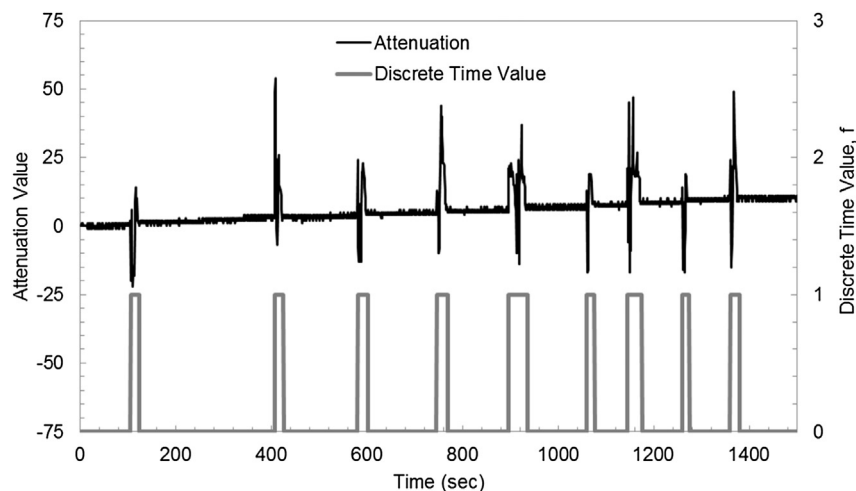


Fig. 5 – Plot of signal attenuation and calculated discrete time fraction over value over time.

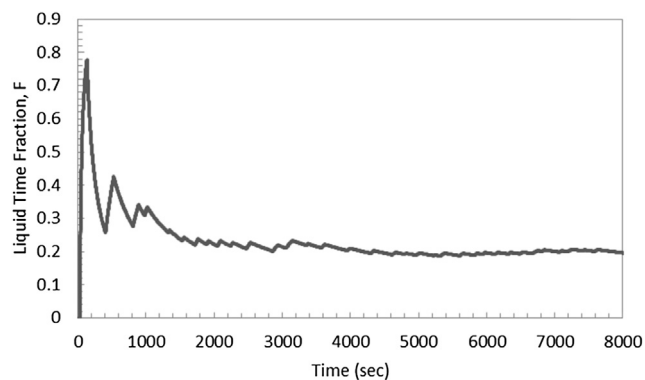


Fig. 6 – Example of liquid time fraction convergence with respect to sample size measured at 1.5 A/cm² and 65% RH.

fuel cell, mostly with regard to the relative humidity. Because of this preliminary testing was performed to characterize the variance of the data over several operating conditions. It was found that the maximum variance occurred under the highest humidity conditions and highest current densities where a high frequency of liquid water detection occurs. Under these conditions a variance of S_1 is calculated and Equation (3) is solved iteratively until the required sample size converges beyond a minimum required value. Given a fixed sample rate of 1 Hz, this then determines the required amount of measurement time at steady state required to approximate a liquid time fraction within the given confidence interval and confidence value.

The maximum required sample size was determined by evaluating a sample size of 10,000 under conditions which yield the greatest standard deviation which was determined to be at an operating voltage of 0.3 V with a relative humidity of 100%. Based on this sample size, and a confidence value of 95% with a confidence interval of ± 0.025 , the minimum required sample size to determine the liquid time fraction was determined to be 4610 sample points. Therefore, a minimal

sample size of 6000 data points, measured over steady state conditions was used to ensure a relatively accurate measurement of the liquid time fraction. Fig. 6 is a plot of the averaged time fraction over time demonstrating how it converges to a single value over time.

Another consideration with regards to confidence and accuracy is sample rate with respect to droplet dwell time. Because the liquid time fraction is a statistical measurement, the sample rate at which water is detected is theoretically irrelevant, assuming an instantaneous sample period. Since the liquid time fraction is the average of the discretely detected water droplets over any given amount of time the sample rate can be at any frequency so long as the criteria for confidence are met. Furthermore, the amount of time at which the measurement is actually taken must be long enough to capture at least one water droplet and one period at which the channel is dry, in other words when the sample standard deviation is not zero. The exception being when the fuel cell is operated under dry conditions and liquid water is not formed.

Experimental setup

The sensor was tested with a single fuel cell consisting of a 7-layer Membrane Electrode Assembly (MEA) with 5 cm² active area. The membrane material used was Nafion NRE-211, with 0.5 mg cm⁻² platinum loadings on the anode and cathode catalyst layers. The GDL material used was Avcarb GDS2120 with a micro-porous layer (MPL). The MEA was ran-in using 12 h of steady state operation at 0.6 V and another 12 h of voltage cycling from open circuit voltage to 0.3 V. The fuel cell was operated using the Fuel Cell Technologies University Fuel Cell Test Bench.

The flow channel plates were machined from POCO AXM-5Q graphite blocks with single serpentine flow channels with a land width of 1 mm, a channel width of 1 mm, and a depth of 1 mm. A single optical sensor was installed in the center of the middle flow channel field on the cathode flow channel plate.

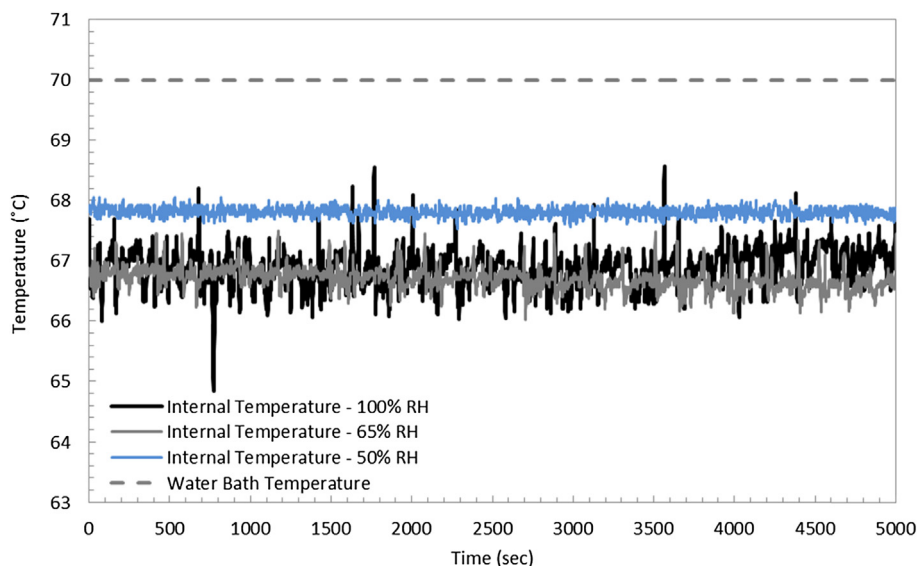


Fig. 7 – Plot of measured internal fuel cell temperature from optical sensor and circulator water bath temperature over time.

Temperature regulation of the cell was achieved through the use of aluminum water blocks placed on the outside of flow channel plates and current collectors. Two separate circulating water baths were used to cycle heated (or cooled) water through the water blocks to maintain a consistent cell temperature. Note that the measured cell temperature is the measured temperature of the water circulating through the water blocks and not a temperature of any of the cell components themselves. Due to heat being removed by natural convection and radiation from the cell to its surrounds, the internal temperatures of the cell will be lower than the circulating water going through it with the exception of when the cell is operating under high load. However, the internal temperature of the cell is being measured by optical sensor. Fig. 7 demonstrates this showing the steady state internal temperature over time measured by the optical sensor at OCV conditions. The internal cell temperature measured by optical sensor is consistently 2–3 °C lower than the water bath temperature, which is surrounding the outside of cell.

Experimental results and discussion

Liquid time fraction as a function of current density and humidity

To characterize the behavior of the fuel cell with regards to water formation in the gas channels the fuel cell was operated at steady state under a range of loads and different relative humidity levels of the reactant gases. The cell was operated at an inlet gas relative humidity of 40%, 65%, and 100% on the anode and cathode. Data from the sensor was recorded at a frequency of 1 Hz over a minimum period of 100 min (6000 samples) for each measurement of the liquid time fraction after the cell had reached steady state. The liquid time fraction as a function of current density is plotted in Fig. 8.

Fig. 8 shows that as the relative humidity of the inlet gases increases so does the time fraction for all operating points as would be expected. As the time fraction increases the water

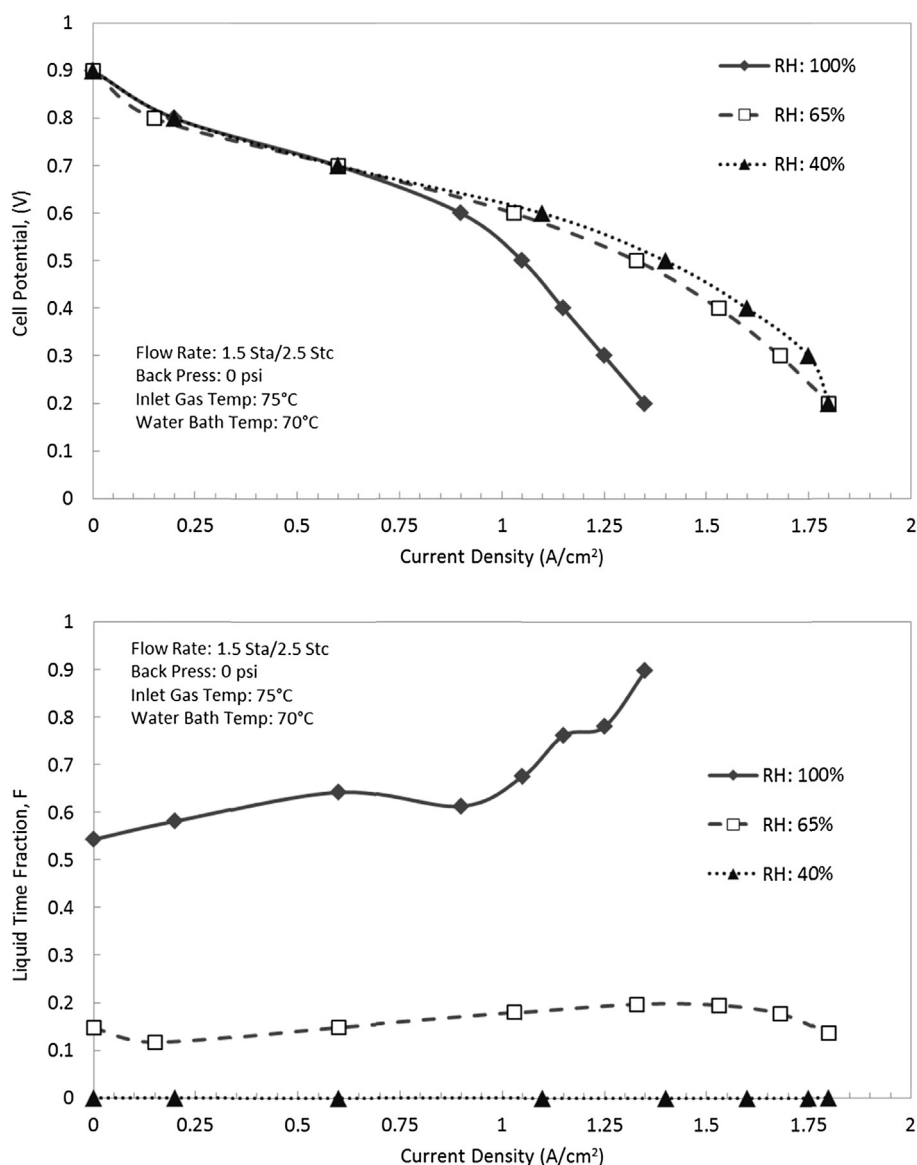


Fig. 8 – Results for liquid time fraction over different reactant gas humidities as a function of current density.

inside the fuel cell experiences greater condensation resulting in more liquid water present in the flow channel. At a relative humidity of 100%, the liquid time fraction never has a value of less than 0.5, which indicates that the channel is typically flooded most of the time, especially at higher current densities. With a time fraction of 0.54 at OCV, water condenses even with no water being produced by the cell. As current density is increased and more water is produced by the cell, the time fraction increases somewhat exponentially until flooding occurs due to the cathode air being completely saturated.

The liquid water formation at OCV is due to the water vapor in the humidified reactant gases condensing as it moves through the cell. This is caused by cold spots in the cell during open circuit or low current operation. Because the cell temperature is controlled by water coolant plates placed on the outside of cell, the temperature at the MEA and flow channel itself is lower than the controlled temperature because of heat loss to the environment. This can be seen in Fig. 7, which shows in situ temperature data of the cell at OCV and shows a lower in situ temperature than the thermal plate temperature.

At a relative humidity of 65% the cell experiences flooding at open circuit voltage as well, although significantly less than what is observed at 100%. The time fraction has a somewhat linear increase with current output until a current density of approximately 1.5 A cm^{-2} is reached at which point the time fraction begins to decrease. The reason for this behavior has yet to be determined but it is assumed to be due to the relationship between current density and internal temperature. At medium current densities the liquid time fraction increases somewhat linearly with current density as would be expected since the increase rate of water production is proportionally greater than water that could be absorbed by evaporation given a constant relative humidity of gas in the flow channel. However, as previous work [21,22] has shown, the internal temperature on the cathode side of a PEMFC increases

exponentially with current density. For a relative humidity of 65%, the temperature measured by the optical sensor recorded a temperature increase of approximately $6 \text{ }^\circ\text{C}$ from a current density of 0 to 1.75 A cm^{-2} . It is hypothesized that this increase in temperature results in a higher saturation pressure of water in the flow channel allowing for a greater amount of evaporation and therefore a reduction in liquid water is observed.

At a relative humidity of 40% the time fraction is always zero regardless of current density. This is due to all water produced being in the vapor form and not condensing because of the low relative humidity.

Relationship between temperature and liquid water

The optical sensor developed in this work allows the temperature to be measured and the liquid water detected simultaneously. When plotted together over time, the relationships between water in the channels and temperature can be observed. Fig. 9 shows a plot of temperature and signal attenuation over time with the cell operating at a constant current density of 1 A cm^{-2} and 65% relative humidity.

At these operating conditions liquid water clearly has an influence on local temperature measured by the sensor. Each instance of liquid water passing through the channel causes the local temperature to rapidly decrease, often by more than $1 \text{ }^\circ\text{C}$, followed by a steady increase back to the steady state temperature. This indicates that the liquid water located in the fuel cell is at a lower temperature than its surrounding components. Since the water droplets are at a lower temperature than the surrounding components this would suggest that evaporation is occurring as the water droplets move through the gas channels. Higher current densities generate more heat within the cell and thereby raising the local temperature. This would cause the saturation pressure to rise encouraging evaporation of liquid water thereby reducing

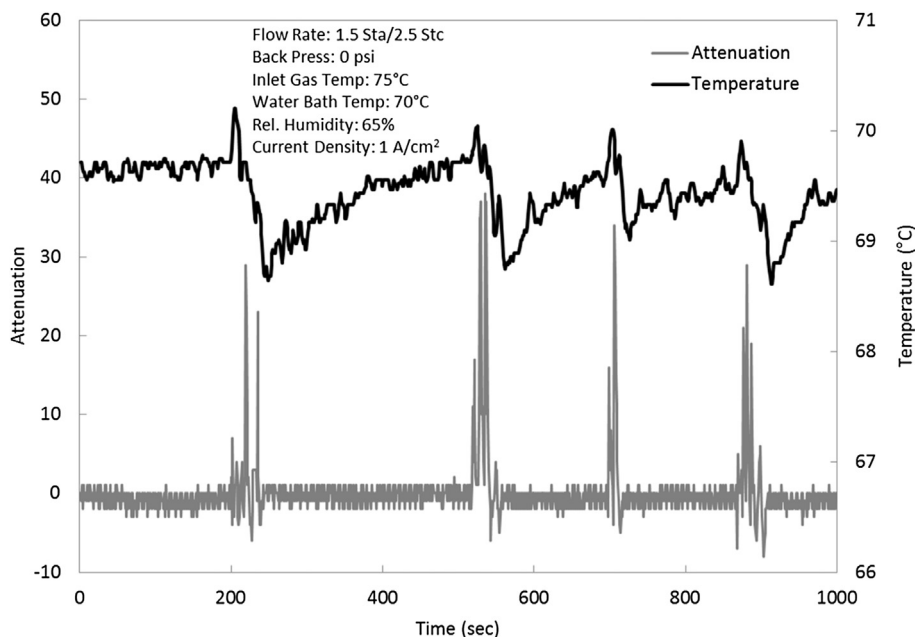


Fig. 9 – Transient plot of temperature and signal attenuation from optical sensor in the cathode PEMFC flow channel.

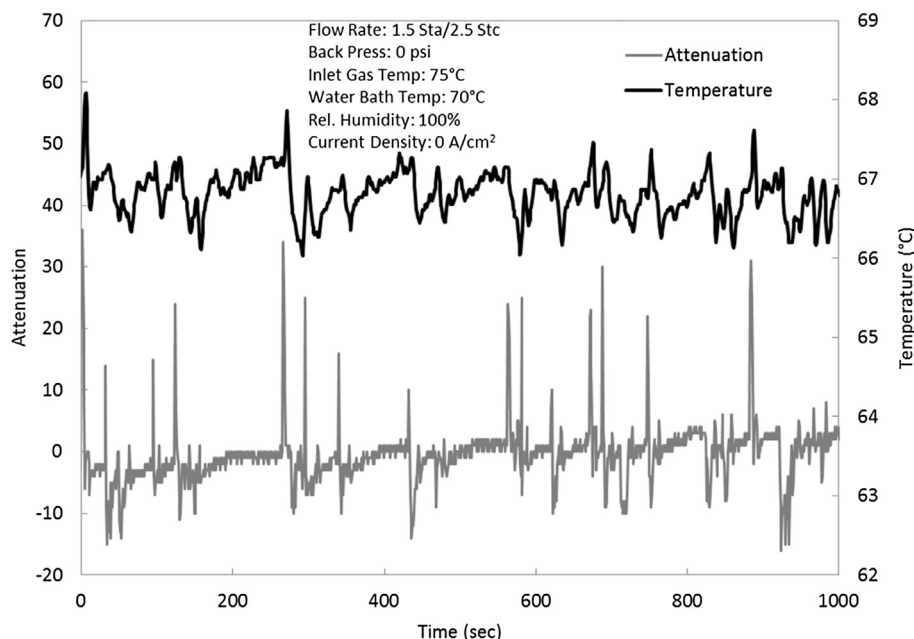


Fig. 10 – Transient plot of temperature and signal attenuation from optical sensor in the cathode PEMFC flow channel.

the droplets temperature. Another possible explanation is due to the temperature difference between the GDL and flow channel plate. It is widely believed that liquid water typically first condenses in the channels of the flow channel plate as it is the coolest surface in the fuel cell's internal environment. This is part of the basis for phase-change-induced flow from the catalyst layer to flow channels. Therefore the water droplets would have a temperature similar to that of the flow channel plate and would be at a lower temperature than the neighboring GDL conducting heat from the catalyst layer. More investigation into this phenomenon is required to determine the actual cause.

Fig. 10 is a transient plot of temperature and attenuation under 100% humidity and open circuit voltage. In this case the relationship between temperature and liquid water is more subtle as the fuel cell isn't generating any heat and the channels are most often flooded. Because the fuel cell is generating no heat or water, all liquid water is formed due to condensation of water from the reactant gases. Liquid water causes both an increase and decrease in temperature and there is no obvious direct relationship.

Conclusions

A method for liquid water detection using an optical temperature sensor was successfully developed. The sensor was implemented in an experimental fuel cell to demonstrate the utility and to characterize the behavior and liquid water formation of the cell along with internal temperature. Furthermore, a method of quantifying the detected liquid was developed by formulating a time fraction which was present in the flow channel.

Results of the experiments presented in this work have shown a relationship between water condensation, relative

humidity, and internal temperature. It assumed that some of this behavior is due to the effects of internal temperature rise changing the saturation pressure of air moving through the gas channels causing greater amounts of evaporation at higher current densities. This effect could possibly be manipulated to aid in decreasing flooding of the cathode.

A relationship between local liquid water formation and temperature was also observed. Under typical operating conditions liquid water clearly has an influence on local temperature and was shown to be at a lower temperature than surrounding components. This would suggest that liquid water is absorbing heat from surrounding components and evaporating as it moves through the flow channel.

Nomenclature

| | |
|----------|----------------------------|
| E | confidence interval |
| N | sample size |
| N_T | total sample size |
| f | discrete time value |
| F | liquid water time fraction |
| S_l | sample standard deviation |
| t | time |
| T | period |
| z_{cv} | confidence value |

REFERENCES

- [1] Conteau D, Bonnet C, Funfschilling D, Weber M, Didierjean S, Lopicque F. Detection of liquid water in PEM fuel cells' channels: design and validation of a microsensor. *Fuel Cells* 2010;9999(9999).

- [2] David NA, Wild PM, Jensen J, Navessin T, Djilali N. Simultaneous in situ measurement of temperature and relative humidity in a PEMFC using optical fiber sensors. *J Electrochem Soc* 2010;157(8):B1173–9.
- [3] Nishida K, Ishii M, Tsushima S, Hirai S. Detection of water vapor in cathode gas diffusion layer of polymer electrolyte fuel cell using water sensitive paper. *J Power Sources* Feb. 2012;199(0):155–60.
- [4] Spornjak D, Prasad AK, Advani SG. Experimental investigation of liquid water formation and transport in a transparent single-serpentine PEM fuel cell. *J Power Sources* Jul. 2007;170(2):334–44.
- [5] Banerjee R, Kandlikar SG. Liquid water quantification in the cathode side gas channels of a proton exchange membrane fuel cell through two-phase flow visualization. *J Power Sources* Feb. 2014;247(0):9–19.
- [6] Sergi JM, Kandlikar SG. Quantification and characterization of water coverage in PEMFC gas channels using simultaneous anode and cathode visualization and image processing. *Int J Hydrogen Energy* Sep. 2011;36(19):12381–92.
- [7] Hussaini IS, Wang C-Y. Visualization and quantification of cathode channel flooding in PEM fuel cells. *J Power Sources* Feb. 2009;187(2):444–51.
- [8] Carton JG, Lawlor V, Olabi AG, Hochenauer C, Zauner G. Water droplet accumulation and motion in PEM (proton exchange membrane) fuel cell mini-channels. *Sustain Energy Environ Prot* 2010 Mar. 2012;39(1):63–73.
- [9] Hartnig C, Manke I, Kardjilov N, Hilger A, Grünerbel M, Kaczerowski J, et al. Combined neutron radiography and locally resolved current density measurements of operating PEM fuel cells Feb. 2008;176(2):452–9. Sel PAP Present. The 10th ULM Electrochem Days W Tillmetz J Lindenmayer.
- [10] Trabold TA, Owejan JP, Jacobson DL, Arif M, Huffman PR. In situ investigation of water transport in an operating PEM fuel cell using neutron radiography: part 1 – experimental method and serpentine flow field results. *Int J Heat Mass Transf* Dec. 2006;49(25–26):4712–20.
- [11] Owejan JP, Trabold TA, Jacobson DL, Baker DR, Hussey DS, Arif M. In situ investigation of water transport in an operating PEM fuel cell using neutron radiography: part 2 – transient water accumulation in an interdigitated cathode flow field. *Int J Heat Mass Transf* Dec. 2006;49(25–26):4721–31.
- [12] Deevanhxay P, Sasabe T, Tsushima S, Hirai S. Observation of dynamic liquid water transport in the microporous layer and gas diffusion layer of an operating PEM fuel cell by high-resolution soft X-ray radiography. *J Power Sources* May 2013;230(0):38–43.
- [13] Bazylak A. Liquid water visualization in PEM fuel cells: a review. *Int J Hydrogen Energy* May 2009;34(9):3845–57.
- [14] Tsushima S, Hirai S. In situ diagnostics for water transport in proton exchange membrane fuel cells. *Prog Energy Combust Sci* Apr. 2011;37(2):204–20.
- [15] Wang Y, Wang C-Y. A nonisothermal, two-phase model for polymer electrolyte fuel cells. *J Electrochem Soc* 2006;153(6):A1193–200.
- [16] Birgersson E, Noponen M, Vynnycky M. Analysis of a two-phase non-isothermal model for a PEFC. *J Electrochem Soc* May 2005;152(5):A1021–34.
- [17] Khandelwal M, Lee S, Mench MM. Model to predict temperature and capillary pressure driven water transport in PEFCs after shutdown. *J Electrochem Soc* Jun. 2009;156(6):B703–15.
- [18] Wang X-D, Xu J-L, Lee D-J. Parameter sensitivity examination for a complete three-dimensional, two-phase, non-isothermal model of polymer electrolyte membrane fuel cell. 2011 Asian Bio-Hydrog. Biorefinery Symp 2011ABBS Oct. 2012;37(20):15766–77.
- [19] Siegel C. Review of computational heat and mass transfer modeling in polymer-electrolyte-membrane (PEM) fuel cells. *Energy Sep.* 2008;33(9):1331–52.
- [20] Ding Y, Bi X, Wilkinson DP. 3D simulations of the impact of two-phase flow on PEM fuel cell performance. 11th Int Conf Gas-Liq. Gas-Liq.-Solid React. Eng. Aug. 2013;100(0):445–55
- [21] Inman K. Design of a non-invasive optical fiber sensor for in situ measurement of temperature in a proton exchange membrane fuel cell. *ECS Trans* 2013;50(2):301–12.
- [22] Inman K, Wang X, Sangeorzan B. Design of an optical thermal sensor for proton exchange membrane fuel cell temperature measurement using phosphor thermometry. *J Power Sources* Aug. 2010;195(15):4753–7.